PCCP

ROYAL SOCIETY OF CHEMISTRY

ARTICLE TYPE

Electronic supplementary information

Supplementary material referred to from the main text is here presented with subsections corresponding to the references.

S1.1 Active space of the RIXS simulations

The partitioning of molecular orbitals into RAS1 (restricted maximum number of electron-holes), RAS2 (no restrictions) and RAS3 (restricted maximum number of electrons) spaces, including the manually imposed permutations of orbital ordering, employed for the RIXS simulations, is shown in Figure S1. The correspondence between O_h and D_{2h} point group denotations is provided in Table S1.

S1.2 GS-NEXAFS spectra of D_{4h} and O_h structures

The (unshifted) GS-NEXAFS spectra of $Fe(CN)_6^{3-}$, extracted from the RIXS simulations, is shown in Figure S2 (a), simulated for the D_{4h} symmetric @GS structure and a structure which was optimized at the same level of theory but with restrictions of O_h symmetry (6 identical Fe-C and 6 identical C-N bond lengths). The spectral differences are insignificant, i.e. far smaller than differences between simulated and measured spectra, and can therefore not be expected to be detectable experimentally.

S1.3 GS-NEXAFS and Quartet-NEXAFS

The (unshifted) NEXAFS spectra of the GS and Quartet state, extracted from the RIXS simulations, are shown in Figure S2 (b). The Quartet spectrum clearly display more complex profiles, as the GS features split into separate sub-features in the Quartet spectrum. To exemplify, we describe in detail the states and transitions which constitute absorption resonance **a**, i.e. $2p \rightarrow 3d(t_{2g})$ x-ray excitation. The analysis is performed in terms of spin-free states (i.e. before spin-orbit interaction), to reduce the number of involved states and simultaneous effects, but still appears to provide reasonable explanation for spectral trends within the specific resonance.

The GS electron configuration has 5 electrons in the t_{2g} shell: $(d_{xy})^1(d_{xz})^2(d_{yz})^2$ and 0 electrons in the e_g shell: $(d_{x^2-y^2})^0(d_{z^2})^0$. This results in two allowed bright degenerate x-ray transitions $(p_x)^{-1}(d_{xy})^{+1}$ and $(p_y)^{-1}(d_{xy})^{+1}$ of high intensity (f=0.282e^{-2}), which together constitute the single feature seen at roughly 714 eV.

The Quartet electron configuration has 4 electrons in the t_{2g} shell: $(d_{xy})^1(d_{xz})^2(d_{yz})^1$ and 1 electrons in the e_g shell: $(d_{x^2-y^2})^0(d_{z^2})^1$. This results in 4 allowed bright x-ray transitions $(p_x)^{-1}(d_{xy})^{+1}$, $(p_y)^{-1}(d_{xy})^{+1}$, $(p_y)^{-1}(d_{yz})^{+1}$ and $(p_z)^{-1}(d_{yz})^{+1}$. Multiplet interactions between the $3d_{z^2}$ electron and the 2p core-hole puts the $(p_z)^{-1}(d_{yz})^{+1}$ transition at roughly 2 eV higher than the others, forming a sub-feature at roughly 715.5 eV; the 3 remaining transitions form a single feature at roughly 713.5 eV. The $(p_x)^{-1}(d_{xy})^{+1}$ transition has a high intensity (f=0.242e^{-2}) comparable to the transitions of the GS-spectrum. The $(p_y)^{-1}(d_{xy})^{+1}$ and $(p_y)^{-1}(d_{yz})^{+1}$ transitions have lower intensity (f=0.106e^{-2} and f=0.133e^{-2} respectively); we ascribe this to configurational mixing in the core-excited state, where the $3d(e_g)$ electron is nearly evenly distributed between the $d_{x^2-y^2}$ and d_{z^2} orbitals, which reduces the overlap with the more purely d_{z^2} occupied initial state. The summed together intensity of the 3 transitions is therefore slightly lower (f=0.481e^{-2}) than of the 2 transitions in the GS spectrum (f=0.564e^{-2}).

S1.4 Fingerprints of electronic and structural effects

The spectra corresponding to Figure 4, but without subtraction of the reference GS-RIXS@GS spectrum, is shown in Figure S3.

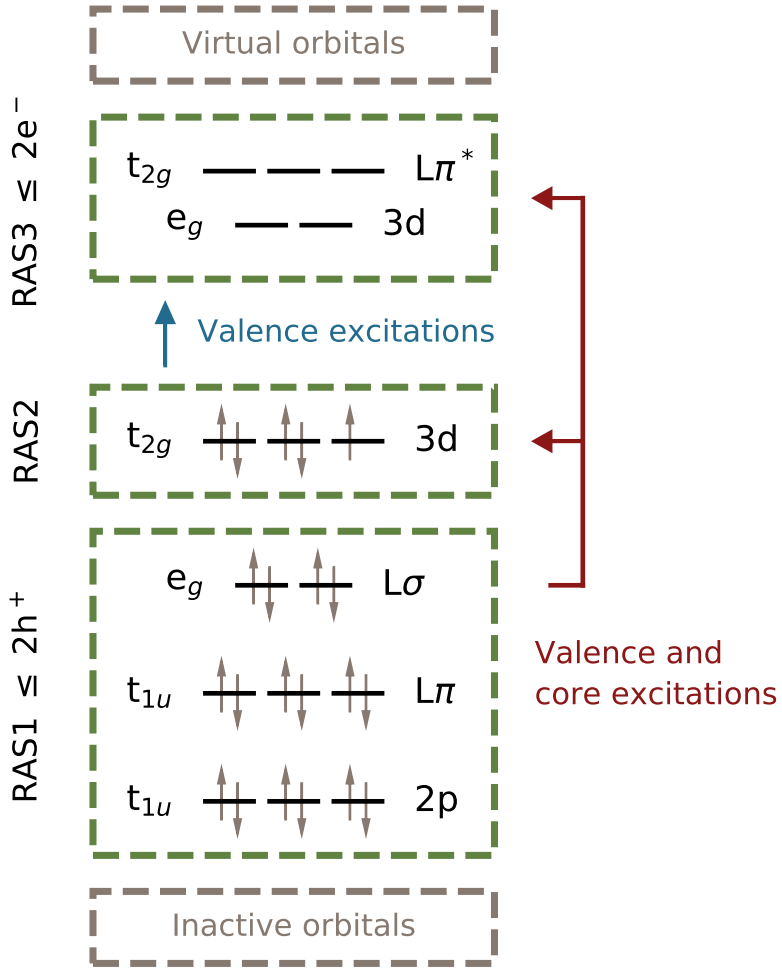

Fig. S1 Active space employed for the RASPT2 RIXS simulations. Core-excitations, LMCT-excitation and final state valence-excitations occur by the creation of up to two electron holes (h^+) in the RAS1 space, and core-excitation and final state valence-excitations by promotion of up to two electrons (e^-) into the RAS3 space.

Orbital	Space	O_h symmetries	D_{2h} symmetries
Lπ^*	RAS3	$3 \times t_{2g}$	$1 \times b_{1g}$, $1 \times b_{2g}$, $1 \times b_{3g}$
3d	RAS3	$2 \times e_g$	$2 \times a_g$
3d	RAS2	$3 \times t_{2g}$	$1 \times b_{1g}$, $1 \times b_{2g}$, $1 \times b_{3g}$
Lπ	RAS1	$3 \times t_{1u}$	$1 \times b_{3u}$, $1 \times b_{2u}$, $1 \times b_{1u}$
Lσ	RAS1	$2 \times e_g$	$2 \times a_g$
Fe2p	RAS1	$3 \times t_{1u}$	$1 \times b_{3u}$, $1 \times b_{2u}$, $1 \times b_{1u}$

Table S1 Table of correspondence between the O_h point group denotation of orbitals utilized in the discussion of results in the main article, and how orbitals are split into D_{2h} symmetries in the RASSCF and RASPT2 calculations.

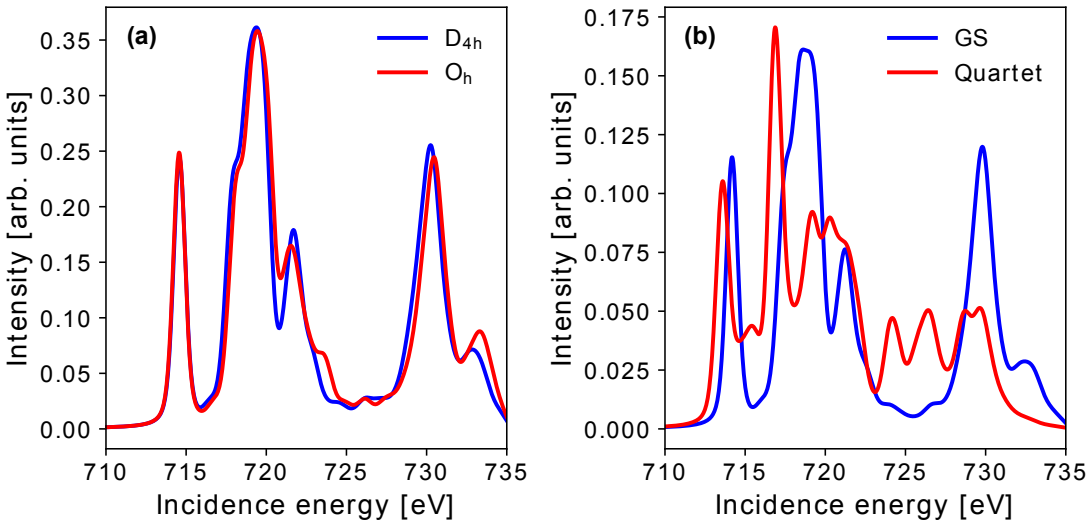

Fig. S2 Simulated near-edge x-ray absorption fine structure (NEXAFS, XAS) spectra of ferricyanide (extracted from the RIXS simulations). **(a)** GS spectrum with the D_{4h} structure utilized for RIXS simulations, compared to GS spectrum with a structure optimized within constraints of O_h structural symmetry. **(b)** GS spectrum vs Quartet spectrum for the D_{4h} symmetric @GS structure.

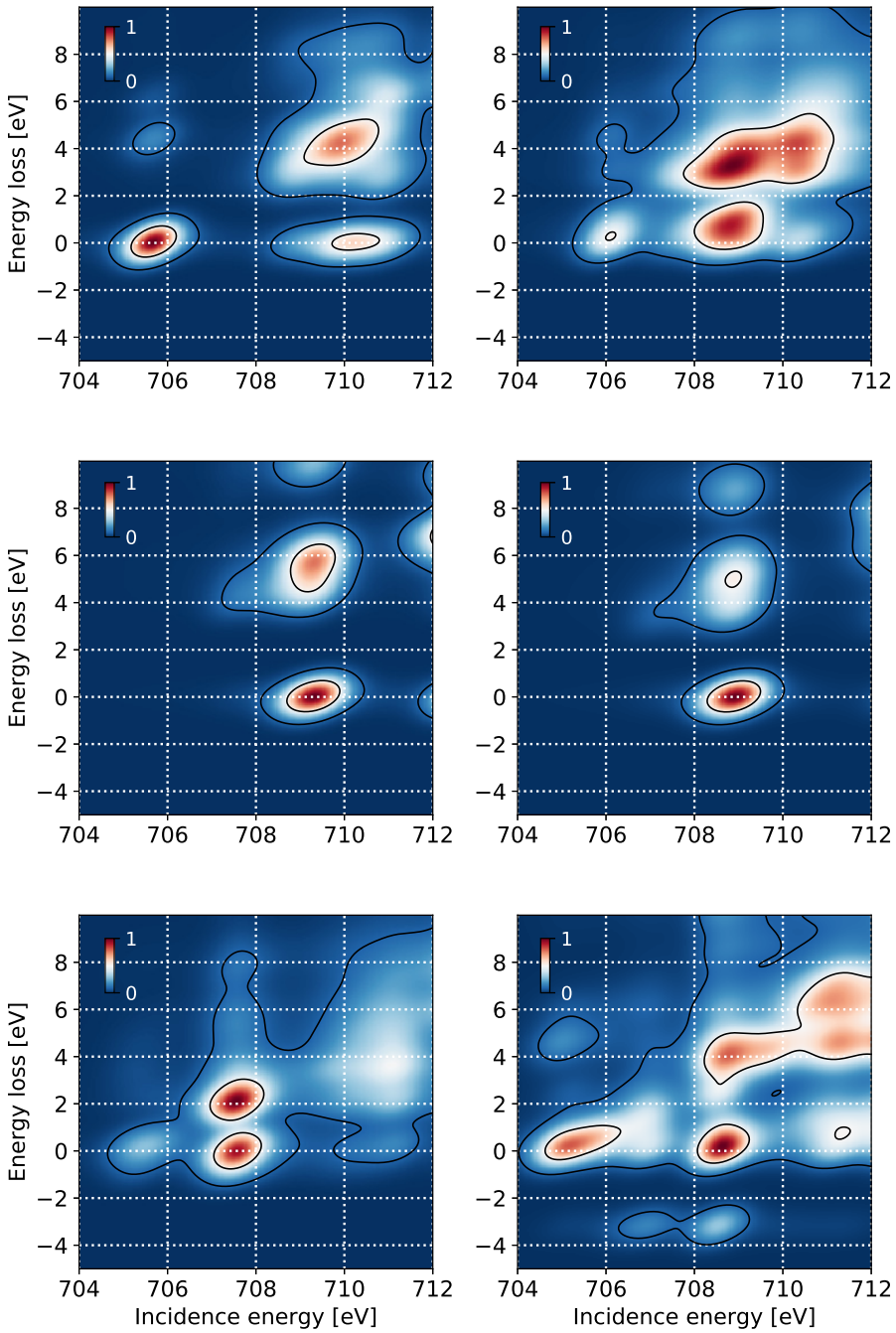

Fig. S3 Combined electronic and structural effects on RIXS spectral features. The figure shows the same spectra as in Figure 4, but with no substraction of the GS-RIXS@GS reference spectrum in the other spectra.